Cure and Physical Properties of Thermoplastic Modified Epoxy Resins Based on Polyethersulfone

ALEXANDER J. MacKINNON,[1] STEPHEN D. JENKINS,[2] PATRICK T. McGRAIL,[2] and RICHARD A. PETHRICK[1,*]

[1]Department of Pure and Applied Chemistry, University of Strathclyde, Thomas Graham Building, 295 Cathedral Street, Glasgow G1 1XL, Scotland and [2]ICI plc, Wilton Research Centre, Wilton, Middlesbrough, Cleveland TS90 8JE, United Kingdom

SYNOPSIS

Dielectric, mechanical, thermal, rheological, and electron microscopy measurements are reported for five series of thermoplastic modified amine cured epoxy resin systems. The epoxy and thermoplastic components have been systematically changed to investigate the factors affecting the phase separation process. Data reported cover both changes in the physical properties occurring during cure and also of the final cured matrix. Dielectric data obtained from fully cured materials exhibits a Maxwell–Wagner–Sillers relaxation process characteristic of a phase separated morphology. Correlation of dielectric relaxation and electron microscopy data indicates that the phase structure changes with the thermoplastic content and composition of the epoxy phase. The mechanical properties change significantly at about 20–25% (w/w) of incorporated thermoplastic, coincident with the formation of a cocontinuous phase morphology. © 1995 John Wiley & Sons, Inc.

INTRODUCTION

Thermoplastic modification of thermoset resin material has been shown to lead to significant improvements in the impact and fracture properties of matrices used in composite manufacture.[1–4] Embrittlement observed in highly crosslinked thermosets[1–8] has restricted their use in carbon fiber composites and has lead to the current interest in toughening materials. Thermoset based resins are preferred for aerospace applications because of their ease of fabrication, low temperatures of cure, high tack, and drape allowing complex shapes to be readily fabricated. Liquid carboxy-terminated butadiene acrylonitrile copolymers (CTBN) are widely used with epoxy resins to generate rubber toughened materials but are subject to degradation at relatively low temperatures. During the curing process, the CTBN rubber phase, which is initially compatible with the components of the resin, separates into micron size domains. The CTBN composite materials have the disadvantage that small amounts of dissolved CTBN molecules reduce the glass transition temperature (T_g) and modulus of the matrix. These resins do not perform very well in hot/wet conditions in comparison to the unmodified thermosets. Linear, high molecular weight thermoplastics are inherently tough and may be expected to reduce the brittleness of a thermoset without degrading other properties. Bucknall and Partridge[2] have used ICI's polyether sulfones in epoxy resin to generate a high temperature thermoplastic modified thermoset. Subsequently, a number of different thermoplastics have been investigated in a range of epoxy resins by Bucknall and Gilbert,[3] Cecere et al.,[4] and Sefton et al.[5] Thermoplastics have also been studied in other types of thermoset networks.[6–8] The thermoplastics and thermosets used in this study were chosen to be thermodynamically compatible; however, it is now recognized that the increasing molecular weight of the thermoset component induces phase separation during the curing process.[9,10] Unlike CTBN that tends to form a simple particulate morphology, the thermoplastic modified epoxy resins may exist as either homogeneous, particulate, cocontinuous, or phase inverted morphologies.[5,8] Application of mi-

* To whom correspondence should be addressed.

Journal of Applied Polymer Science, Vol. 58, 2345–2355 (1995)
© 1995 John Wiley & Sons, Inc. CCC 0021-8995/95/132345-11

croprocessor control to dielectric measurement[11-17] has enabled real time observation of the dipolar relaxation characteristics of thermosets undergoing cure. Previous studies of the cure of epoxy/thermoplastic blends[18-20] indicated that the final physical properties depend critically on the amount of thermoplastic present.

Polarization occurs in heterogeneous dielectrics as a result of accumulation of charge at the interfaces between media having differing conductivities. The observed dielectric dispersions associated with polarization in such systems can be several orders of magnitude larger than those typically observed for dipolar relaxation. The dielectric theory describing these Maxwell–Wagner–Sillers (MWS) processes has been reviewed by van Beek[21] and was discussed in previous publications.[18-20]

This article considers the effect of systematically altering the epoxy and thermoplastic components on the morphology, dielectric, thermal, rheological, and mechanical properties of these systems.

EXPERIMENTAL

Materials

Two thermoset systems were investigated: triglycidylaminophenol (Ciba Geigy, MY0510), cured with 4,4′-diaminodiphenylsulfone (4,4′-DDS, Ciba Geigy HT976); and a 1 : 1 (w/w) mixture of diglycidylether of bisphenol F (Ciba-Geigy PY306) and MY0510 cured with 4,4′-DDS.

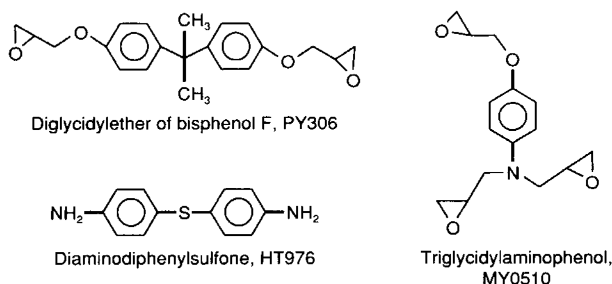

Diglycidylether of bisphenol F, PY306

Diaminodiphenylsulfone, HT976

Triglycidylaminophenol, MY0510

The epoxy resin and hardener were used as supplied in the ratio of 2.1 : 1 (w/w). The thermoplastics (TP) incorporated are shown in Table I. Cured sheets were made by dissolving the thermoplastic in a 95 : 5 (v/v) mixture of methylene chloride and methanol and adding the appropriate amount of epoxy and hardener before the solvent was evaporated off, leaving a homogeneous solution. The blend was poured into an open mold (dimensions 14 × 10 cm) preheated to 140°C and degassed for 30 min under vacuum to remove residual solvent and trapped air. For studies of the curing process the mold was removed from the oven and cooled rapidly and stored at −20°C until used. Samples were also cured at 180°C for a further 120 min and then cooled to room temperature over a period of 120 min. A range of samples with varying thermoplastic content (0–40% w/w) were made for each thermoset system. Five series of blends were prepared and the system number and composition are designated as follows:

1. MY0510/4,4′-DDS/5003P
2. MY0510/4,4′-DDS/RT-PS(A)
3. MY0510/4,4′-DDS/RT-PS(B)
4. MY0510/PY306/4,4′-DDS/RT-PS(A)
5. MY0510/PY306/4,4′-DDS/RT-PS(C)

Dielectric Measurements

Measurements were performed using a Solartron 1250 frequency response analyzer operating between 0.1 and 6×10^5 Hz. The frequency range was selected to achieve collection of 30 data points within a period of 3 min. The time taken typically for cure of the resin at 180°C was 100 min, hence the data collection time is sufficiently short to approximate to an instantaneous snapshot of the dielectric properties of the system. Two pre-etched copper electrodes mounted on an epoxy glass fiber base separated by a copper spacer were used to form the cell for these experiments. A three terminal electrode system with area of 1 cm^2 maintained constant separation by soldering the copper spacer around three edges of

Table I Thermoplastic Incorporated in Study Resins

Code Name	Description of Polyethersulfones	Number Average Molar Mass − M_n	Viscosity Index − R_v
Victrex 5003P	Polyethersulfone	24000	0.50–0.52
RT-PS(A)	Amine terminated polyethersulfone	11000	0.20–0.28
RT-PS(B)	Epoxidized polyethersulfone	13000	0.24–0.28
RT-PS(C)	Amine terminated polyethersulfone	13000	0.24–0.28

the cell. The cell was designed to allow overfilling to accommodate shrinkage of the resin on cure. Depending on the viscosity the initial mixture was either heated and poured into the cell or alternatively a solid piece was cut from the frozen pre-plaque and inserted between the electrodes before cell construction was completed. The cell was placed in a modified heating block of an Oxford Instruments cryostat (DN1704) and isothermal conditions were maintained using an Oxford Instruments ITC4 temperature controller. The method used for the dielectric measurements were described previously.[18]

Rheological Measurements

A curometer, designed at Strathclyde, was used to monitor changes in the viscosity as a function of time and allowed determination of the real and imaginary parts of the shear modulus at 2 Hz.[22] The instrument was calibrated using a Santovac-5 that exhibits a high temperature–viscosity coefficient and forms a stable supercooled liquid state.[23,24]

Electron Microscopy Investigations

Scanning electron microscopy (SEM) micrographs were obtained using an Hitachi S-520 SEM. Samples were prepared for examination by polishing with alumina and then etched with a 1% solution of potassium permanganate in a 5 : 2 : 2 volume mixture of concentrated sulfuric acid : phosphoric acid : distilled water. After etching the samples were sequentially washed in aqueous sulfuric acid, hydrogen peroxide (100 vol), water, and finally acetone. All samples were then sputter coated with gold before SEM examination.

Differential Scanning Calorimetry (DSC) Measurements

DSC measurements were conducted using a Du Pont model 9900 DSC. Samples of approximately 10 mg were heated at a rate of 10°C/min from 30 to 300°C. The first heating scan was used to calculate the heat of reaction, the sample was then allowed to cool to room temperature over a period of 60 min, and a second scan used to determine the final glass transition temperature.

Mechanical Testing

Molded plaques were used to produce samples for the following mechanical tests: Flexural modulus: a 3-point bend test was carried out at 5 mm min^{-1} using a sample size of 50 × 10 × 3 mm; yield strength σ_y: measured in compression mode using a sample size of 10 × 10 × 3 mm; crack opening mode stress intensity factor, K_{Ic}, measured at 1-mm min^{-1} using a sample size of 70 × 10 × 3 mm with a single edge notched on the 10-mm face; and strain energy release rate for opening mode, G_{Ic}, at 1 mm min^{-1} using a sample size of 70 × 10 × 3 mm with a single edge notch on the 10-mm face. All measurements were made at 23°C. In addition, the ductility factor, $(K_{Ic}/\sigma_y)^2$, was derived from the measurements.[25]

RESULTS AND DISCUSSION

Curometer Data

The time dependence of the viscosity of the mixtures with varying thermoplastic content were examined using the Strathclyde curometer. The gelation point is taken as the time at which the viscosity reaches a value of 10^4 Pas (Table II). Addition of thermoplastic to the thermoset matrix inhibits the cure and it was not possible to investigate systems containing less than 20% thermoplastic at 180°C due to the highly exothermic nature of the cure process. At higher thermoplastic content the polymer acts as a diluent, inhibiting the reaction and reducing the rate at which heat is liberated. The functionally terminated thermoplastics show shorter cure times than the corresponding nonfunctionalized resin; however the use of a trifunctional epoxy resin inhibits gelation. The epoxy terminated thermoplastic enhances gelation more than the corresponding amine terminated resin. These observations are consistent with the anticipated reactivities of these groups and the effects of functionality on the topology of the growing network structure.

DSC Measurements

The curing exotherm was determined for the mixture by DSC analysis. The T_g was obtained from mea-

Table II Gelation Data

Thermoplastic (wt %)	System Time (min)				
	1	2	3	4	5
20.6	23.4	N/A	N/A	19.8	N/A
26.7	28.5	23.3	20.0	28.8	23.8
30.0	31.0	28.8	23.7	40.2	25.8
34.6	34.7	34.7	27.0	39.3	41.8
39.1	36.0	46.3	35.0	56.0	58.5

Table III DSC Data

	System 1		System 2		System 3		System 4		System 5	
TP (wt %)	T_g (°C)	ΔH (J g^{-1})	T_g (°C)	ΔH (J g^{-1})	T_g (°C)	ΔH (J g^{-1})	T_g (°C)	ΔH (J g^{-1})	T_g (°C)	ΔH (J g^{-1})
0.0	237.3	666.7	237.3	666.7	237.3	666.7	191.3	599.9	191.3	599.9
5.4	220.0	624.0	227.1	700.7	217.7	621.5	182.1	521.8	187.3	507.0
11.0	217.3	618.4	217.6	594.1	210.8	536.2	185.3	468.7	181.0	445.0
15.6	214.3	566.6	202.6	555.1	194.3	438.4	182.4	458.9	188.3	421.6
20.6	206.7	483.2	188.0	506.5	181.9	530.1	184.9	407.7	168.9	358.8
26.7	212.4	475.6	207.0	415.2	192.3	549.4	179.4	397.5	182.1	340.1
30.0	215.0	448.7	208.3	431.8	214.1	476.2	180.9	395.0	183.6	373.0
34.6	213.8	444.8	199.9	386.4	193.7	450.3	183.0	330.0	174.8	323.2
39.1	209.4	412.6	191.5	393.3	194.5	417.2	183.2	306.0	185.3	298.8

surements on the completely cured material (Table III). The curing exotherm decreased linearly with increase in the thermoplastic content and no significant deviations from simple additivity were observed. In this system, T_g of the uncured epoxy resin material differs significantly from that of the epoxy/thermoplastic blends. Due to the close proximity of the T_gs of the individual components, a single value was observed that did not vary significantly with composition.

Electron Microscopic Examination

Electron micrographs were obtained for the various blends and have been reported previously[20] (Fig. 1), and all the materials containing thermoplastic ex-

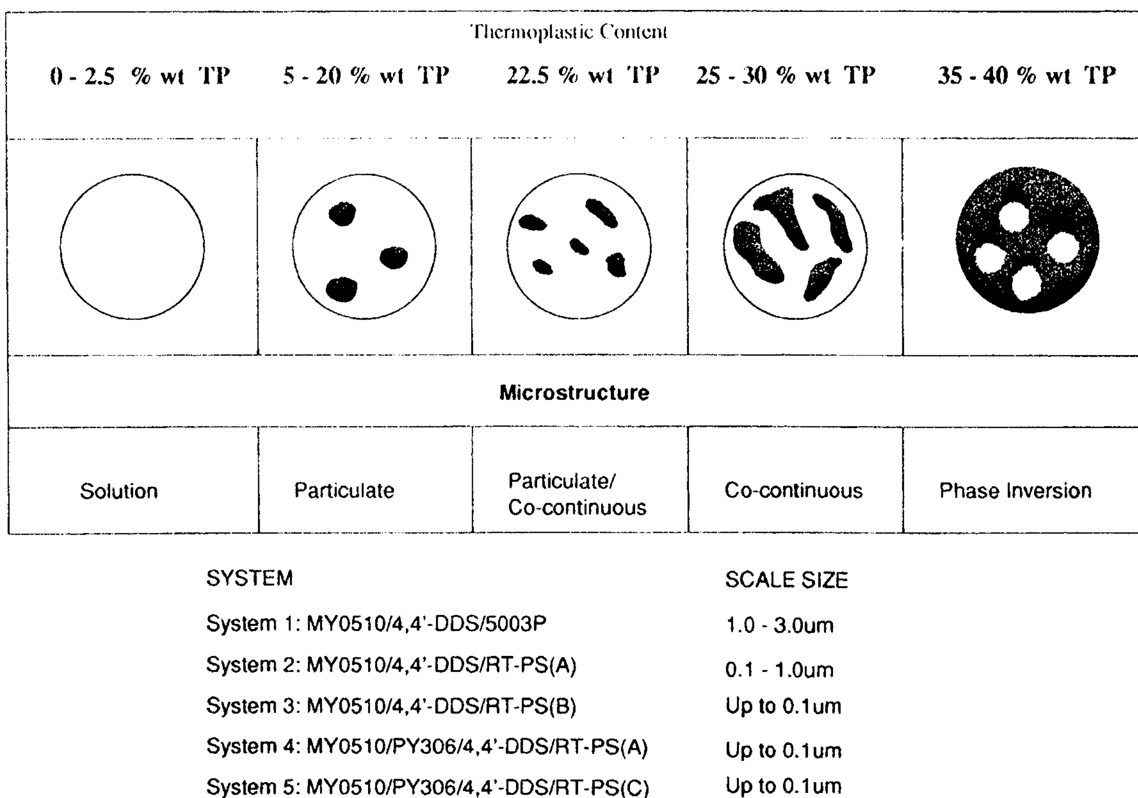

Figure 1 Schematic diagram of microstructures of systems 1–5 as a function of thermoplastic content (Source: ICI plc).

hibited phase separated morphology. Below 20%, the occluded phase is thermoplastic rich and an increase in the thermoplastic content changes the occlusions from spherical to ribbonlike and ultimately a co-continuous phase is generated at a composition of approximately 20–25%. At higher levels of thermoplastic, a phase inverted structure is generated with the occluded phase now being epoxy rich. The composition of the blends has a significant effect on the size of the occlusions. System 1, containing 5003P, shows the largest scale size ranging from 1.0 to 3.0 μm. Introduction of the lower molecular weight RT-PS(A) in place of 5003P induces the formation of finer morphologies with sizes in the region of 0.1–1.0 μm. The replacement of RT-PS(A) with RT-PS(B) had the effect of producing sizes an order of magnitude lower. This change can be attributed to a change in the functionality of the end groups rather than changes in molecular weight. The introduction of a second epoxy component, PY306, to the thermoset matrix of system 2 to produce system 4 induces a further drop in size by an order of magnitude.

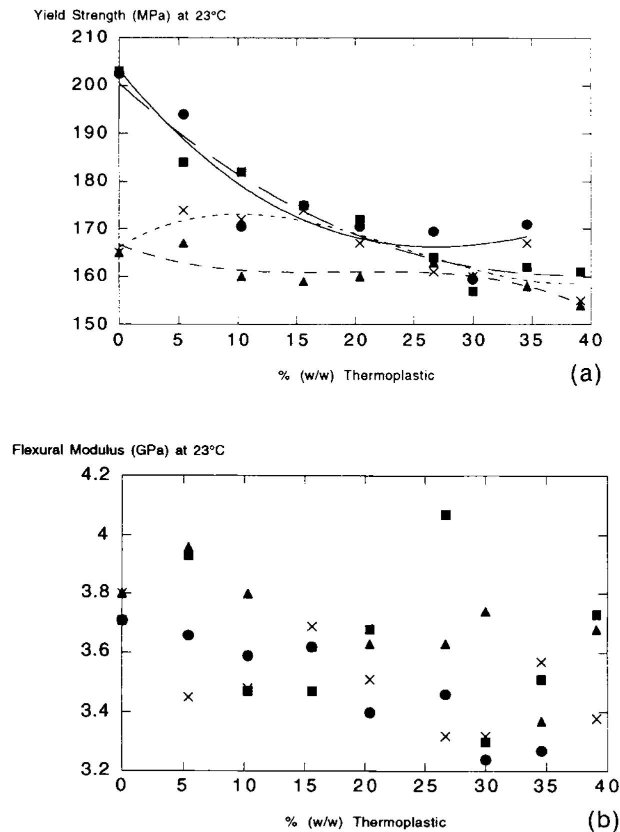

Figure 2 Mechanical data for the five systems: (a) yield strength as a function of composition, (b) flexural modulus (GPa), (c) G_{Ic} (kJ m^{-2}), (d) K_{Ic} (MN m$^{-3/2}$), and (e) ductility factor (μm); all measured at 23°C.

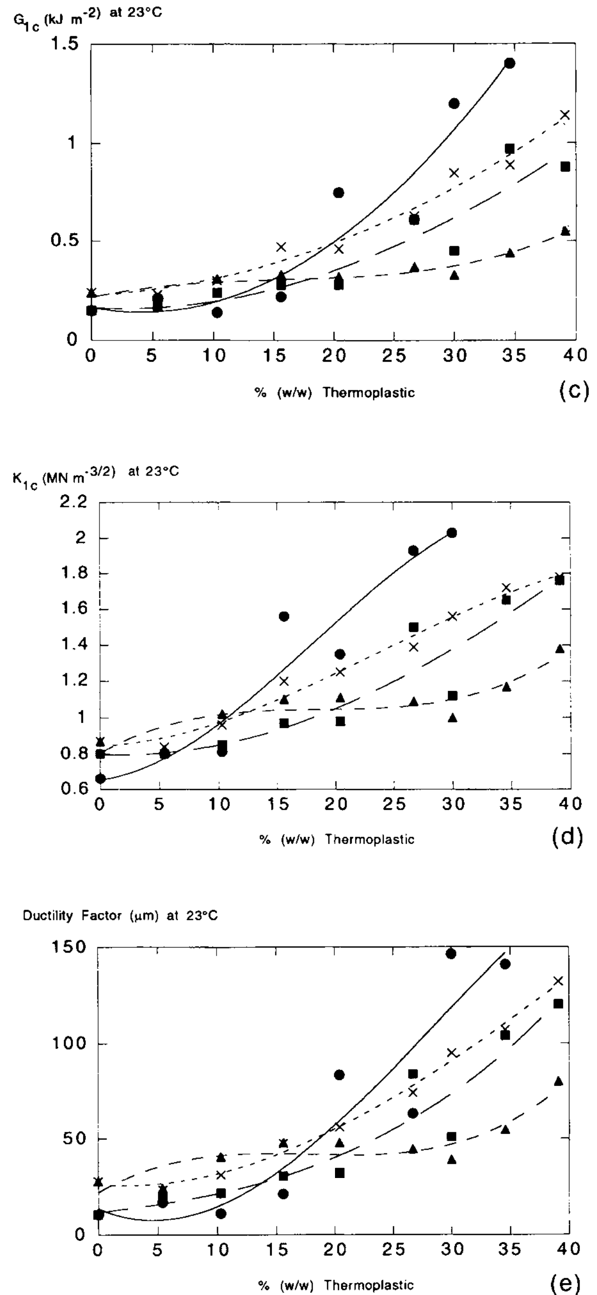

Figure 2 (*Continued*)

Mechanical Testing

Mechanical properties of the blends, with the exception of system 3 that because of insufficient quantities of RT-PS(B) could not be investigated, are shown in Figure 2(a–e). The flexural modulus data shows a progressive decrease with increase in thermoplastic content for system 1 but the remaining systems show little correlation. The introduction of PY306 cause an increase in the flexural modulus

of the unmodified epoxy system. The yield strength shows a dependence on thermoplastic content for all four systems. Systems 1 and 2 resemble one another at corresponding thermoplastic levels with a distinct leveling off at 20–25% content and is consistent with the thermoplastic becoming the dominant phase in the matrix. No specimens of system 2 at the highest thermoplastic content were available. In the case of other modified epoxy resin systems, and in particular those containing CTBN, the inclusion of a rubber will lower the mechanical strength of the material.[3,26,27] The introduction of a second epoxy component into the thermoset matrix causes a significant decrease in yield strength at low thermoplastic contents indicated by comparing system 2 with 4. Above 20% thermoplastic content, the yield strengths for all four systems are reasonably similar reflecting the dominance of the thermoplastic phase. There is little evidence of a progressive change in yield strength for systems 4 and 5. Considering the fracture toughness properties (K_{Ic} and G_{Ic} data), all four series show similar trends with a

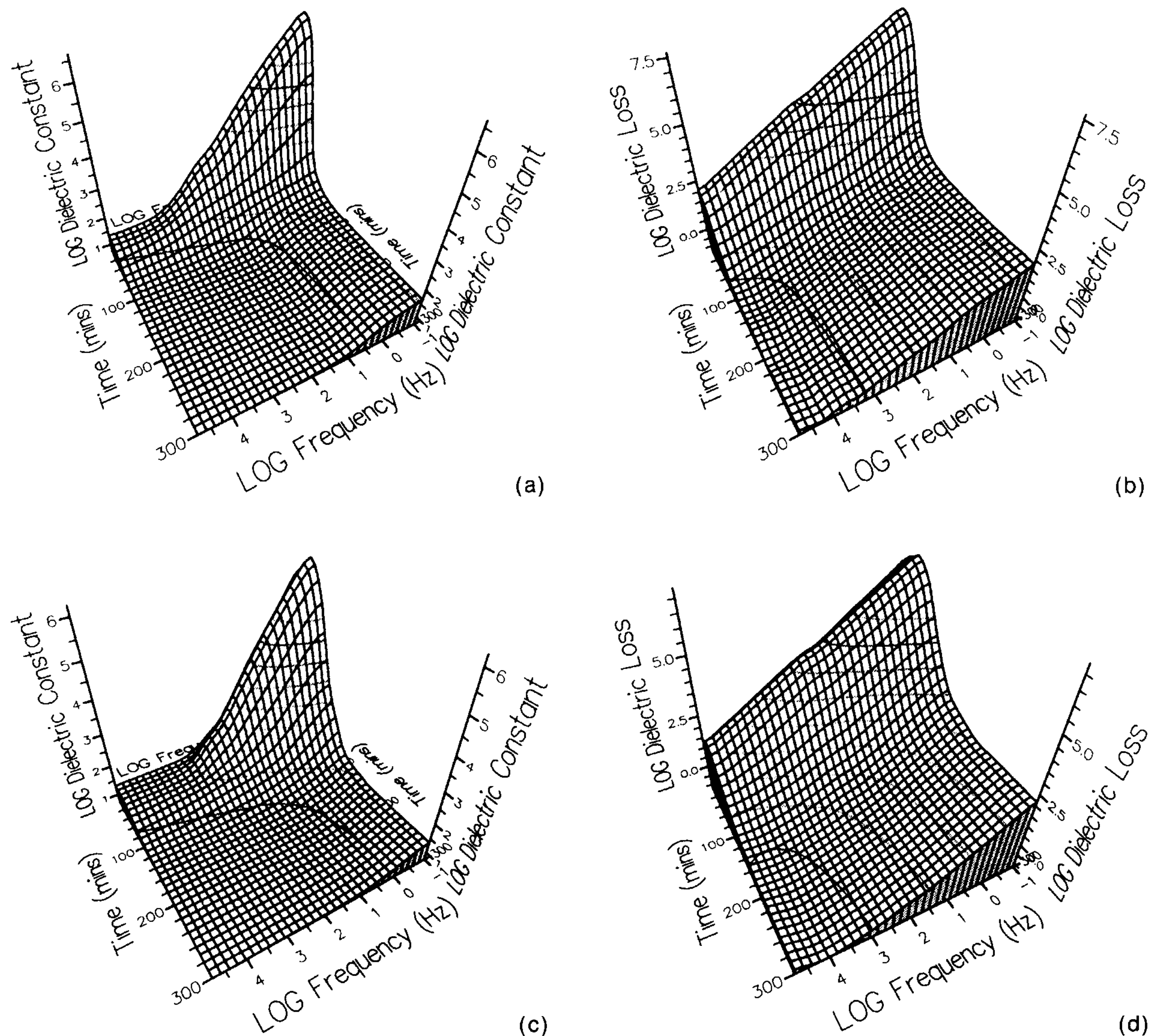

Figure 3 Examples of real time dielectric traces measured at 180°C: (a) Dielectric constant, (b) dielectric loss for MY0510/4,4′-DDS/30% 5003P, (c) Dielectric constant, (d) dielectric loss for MY0510/4,4′-DDS/30%/RT-PS(A), (e) Dielectric constant, (f) dielectric loss for MY0510/4,4′-DDS/30%/RT-PS(B), (g) Dielectric constant, (h) dielectric loss for Bis F/MY0510/4,4′-DDS/30% RT-PS(A), (i) Dielectric constant, (j) dielectric loss for Bis F/MY0510/4,4′-DDS/30% RT-PS(C).

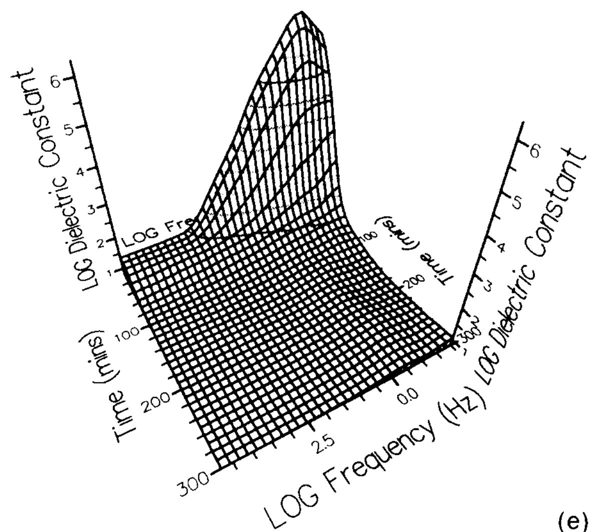

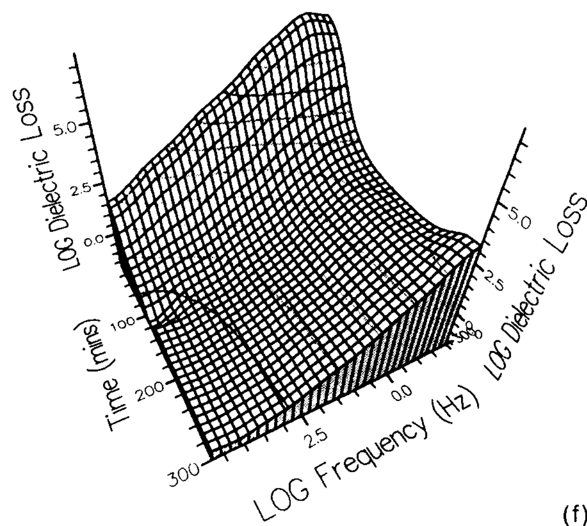

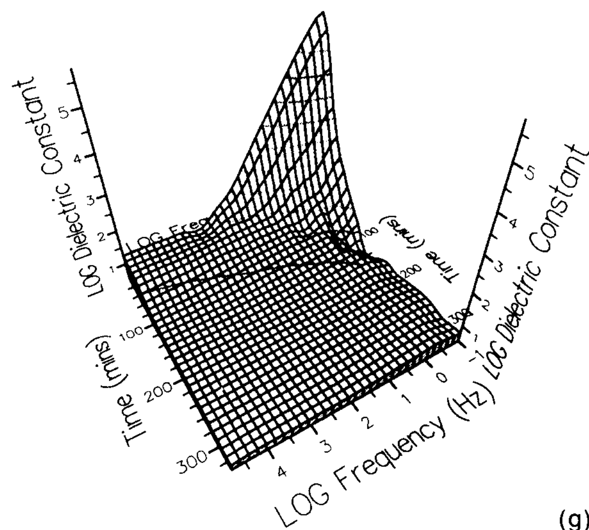

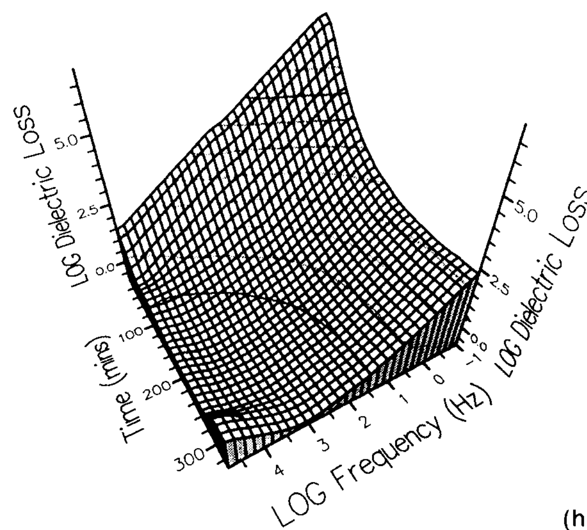

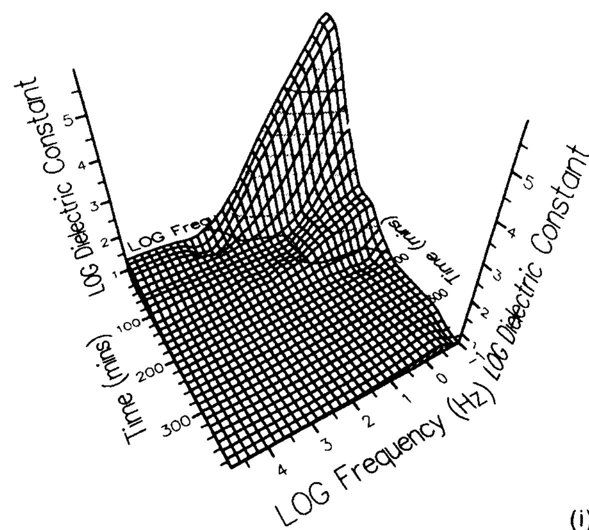

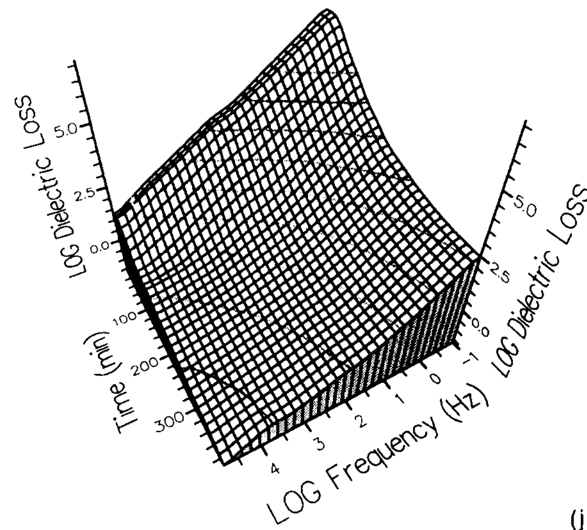

Figure 3 *(Continued)*

significant increase in the fracture toughness at ~ 20% thermoplastic content consistent with formation of a cocontinuous matrix. The 5003P blend shows a greater degree of toughening consistent with the relatively high molecular weight of the thermoplastic. System 4 that incorporates RT-PS(A) shows the least improvement in fracture toughness, and no significant increase in K_{Ic} and G_{Ic} at the point of formation of a cocontinuous matrix. Incorporation of RT-PS(C) instead of RT-PS(A) causes a vast improvement in the fracture toughness above 20% thermoplastic. The only difference in the two thermoplastics is that RT-PS(C) is a slightly higher molecular weight version of RT-PS(A) both having similar functionality. Similar trends are obtained for the ductility factor data.

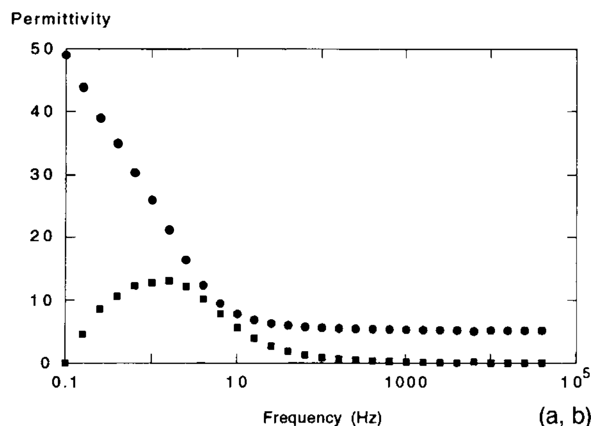

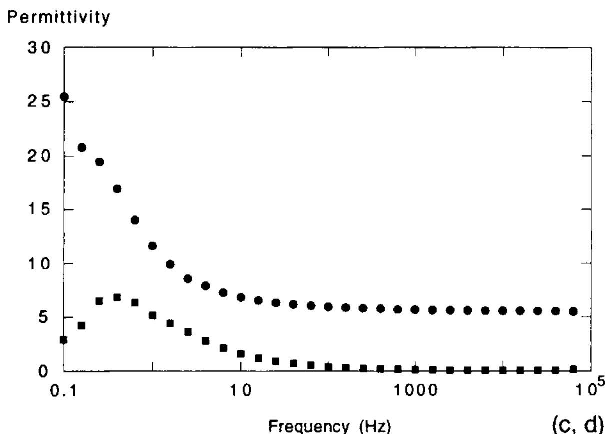

Figure 4 Examples of the final traces for the five resin systems: (a) Dielectric constant, (b) dielectric loss for MY0510/4,4'-DDS/30% 5003P, (c) Dielectric constant, (d) dielectric loss for MY0510/4,4'-DDS/30%/RT-PS(A), (e) Dielectric constant, (f) dielectric loss for MY0510/4,4'-DDS/30%/RT-PS(B), (g) Dielectric constant, (h) dielectric loss for Bis F/MY0510/4,4'-DDS/30% RT-PS(A), (i) Dielectric constant, (j) dielectric loss for Bis F/MY0510/4,4'-DDS/30% RT-PS(C).

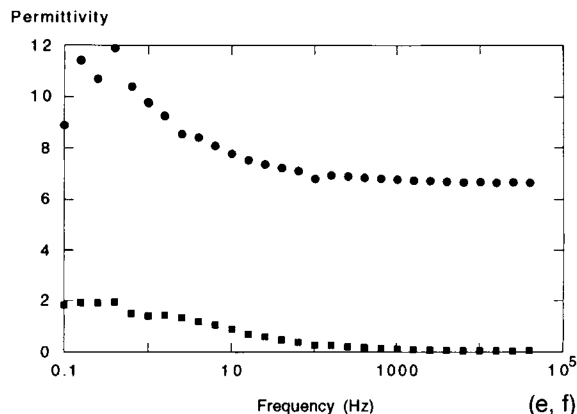

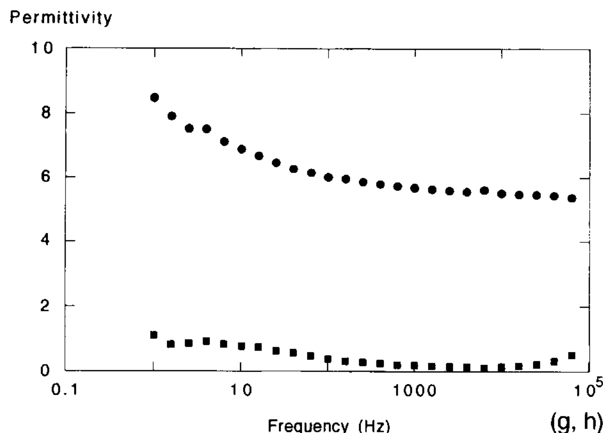

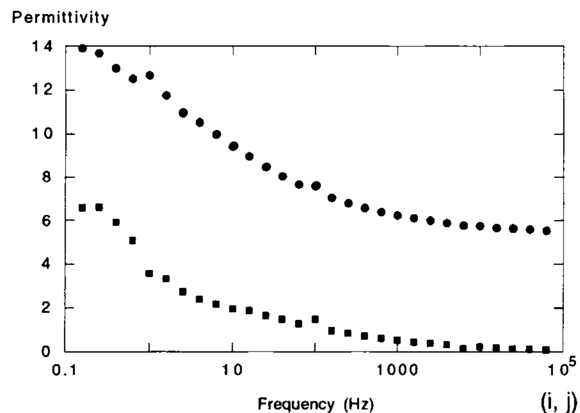

Figure 4 (*Continued*)

Dielectric Measurements

Isothermal cure measurements were performed at 180°C as a function of the composition of thermoplastic over the frequency range 10^{-1}–10^5 Hz. The

Table IV Dielectric Properties at 180°C of Cured System 1

Thermoplastic (wt %)	ε'_{∞}	$\Delta\varepsilon$	σ'_{dc} (Ω^{-1} m^{-1}) $\times 10^{-9}$
0.0	8.6	4.0	4.70
5.4	5.1	3.4	4.71
11.0	4.6	1.4	2.63
15.6	8.6	2.9	5.00
20.6	7.8	4.6	4.00
26.7	5.3	57.3	0.808
30.0	5.1	43.9	0.436
34.6	4.2	24.6	0.164
39.1	3.8	15.7	0.128

Table VI Dielectric Properties at 180°C of Cured System 3

Thermoplastic (wt %)	ε'_{∞}	$\Delta\varepsilon$	σ'_{dc} (Ω^{-1} m^{-1}) $\times 10^{-9}$
0.0	8.4	4.0	4.7
5.4	7.3	6.9	1.86
11.0	6.5	4.2	0.372
15.6	7.5	5.7	2.66
20.6	8.8	6.1	1.13
26.7	4.6	2.1	1.71
30.0	6.6	3.4	1.05
34.6	6.7	5.7	0.551
39.1	6.1	3.9	0.466

three-dimensional plots for the 30% thermoplastic/epoxy blend are shown in Figure 3(a–j) for each of the five systems. Three distinct relaxation features can be identified. At low frequency and short times, a large dielectric loss is evident that rapidly decreases as cure proceeds, and this is attributed to blocking electrode effects.[24,26] A high level of dc conductivity, characterized by an approximate −1 slope of ($\delta \log \varepsilon''/\delta \log f$), is observed initially and this is reduced during cure but is still clearly evident in the fully cured matrix. The dipolar relaxation, observed as a peak in the loss at high frequencies and an increment in the dielectric constant, disappears after approximately 100 min and is associated with vitrification of the matrix.

The dielectric spectrum of the cured material contains two features: first, a contribution to the loss associated with dc conductivity and second, a loss process only observed in the higher thermoplastic content materials. This latter process is attributed to polarization of the occluded phases, the MWS effect. The dc conductivity process does not contribute to the dielectric constant data whereas the MWS effect does. An SEM examination of these materials indicates a systematic variation of the morphology with thermoplastic content (Fig. 1). At low thermoplastic contents, a particulate morphology is observed, the occluded phase being thermoplastic rich. Correlation of the morphology obtained from the SEM study with variation in the dielectric properties indicates that the MWS feature only occurs with the cocontinuous or phase inverted morphology. The MWS model requires the occluded phase to have a higher conductivity than the surrounding matrix and for a large amplitude should approximate to an oblate spheroid. Prediction of permittivity using MWS theory has been discussed in previous publications.[18–20]

To separate the MWS feature from the conductivity, it is necessary to subtract from the loss a

Table V Dielectric Properties at 180°C of Cured System 2

Thermoplastic (wt %)	ε'_{∞}	$\Delta\varepsilon$	σ'_{dc} (Ω^{-1} m^{-1}) $\times 10^{-9}$
0.0	8.6	4.0	4.70
5.4	5.6	3.0	0.823
11.0	8.3	5.7	0.144
15.6	7.6	5.2	2.52
20.6	3.0	11.3	0.112
26.7	7.8	17.8	1.78
30.0	5.5	20.0	0.437
34.6	5.8	20.3	0.247
39.1	6.2	23.1	0.229

Table VII Dielectric Properties at 180°C of Cured System 4

Thermoplastic (wt %)	ε'_{∞}	$\Delta\varepsilon$	σ'_{dc} (Ω^{-1} m^{-1}) $\times 10^{-9}$
0.0	7.4	0.1	1.43
5.4	6.2	4.0	1.20
11.0	5.4	4.8	2.56
15.6	5.6	3.9	1.25
20.6	7.1	4.2	0.99
26.7	7.0	8.8	1.16
30.0	5.4	4.0	1.69
34.6	5.9	6.7	1.50
39.1	6.7	19.0	6.48

Table VIII Dielectric Properties at 180°C of Cured System 5

Thermoplastic (wt %)	ε'_{∞}	$\Delta\varepsilon$	σ'_{dc} $(\Omega^{-1}\ m^{-1}) \times 10^{-9}$
0.0	7.4	0.1	1.43
5.4	6.2	1.6	0.358
11.0	6.2	1.1	1.31
15.6	6.9	3.2	2.74
20.6	6.1	2.8	1.27
26.7	6.3	3.8	1.45
30.0	5.7	4.2	1.70
34.6	5.4	5.4	2.12
39.1	5.2	5.8	1.80

contribution that varies according to $1/\omega$. Figure 4(a–j) illustrates the application of the subtraction process; the resultant dielectric loss curve is significantly broader than would be predicted by the simple Debye process indicating a distribution of relaxation processes consistent with a distribution in the morphological structure. Detailed analysis of the position and amplitude of this process indicates significant variation with composition of the thermoplastic. The MWS feature was observed once the thermoplastic levels were greater than 20.6%. Systems 1 and 2 produce the most distinct dielectric features, with a step in the dielectric constant and a peak in the dielectric loss. Systems 3, 4, and 5 do not produce distinct dielectric loss peak and the magnitude of the loss is considerably lower. The lack of an observable MWS feature is a consequence of the low conductivity and the small size of the occlusions. The dielectric characteristics for each system are illustrated in Tables 4–8 and indicate that only for system 1 is a simple correlation with thermoplastic content observed. In the other systems complex variations in the form of the MWS feature occur reflecting changes in the size, distribution, and volume fraction of occlusions in the final thermoset material.

CONCLUSIONS

Dielectric spectroscopy has been demonstrated as an effective technique in the study of the cure of thermoplastic modified epoxy resins in two distinct ways. First, in a dynamic sense, it was possible to monitor the cure from the initial stages through the vitrification process and finally through to the fully cured state. Second, the dielectric measurements can be correlated with the microstructure of the thermosets. The principle difference between the systems containing RT-PS(B) and RT-PS(C) is the end group functionality, whereas that between RT-PS(A) and RT-PS(C) is a small change in the molecular weight. It is known that the morphology is sensitive to molecular weight and it is probable that variations in the phase size reflect small amounts of higher molecular weight components that do not significantly affect the observed values of the average values of M_n. The variation in the MWS peak observed in the dielectric spectra of the fully cured materials is consistent with the fact that in moving from system 1 to system 2 there is an increase in the average size and a reduction in the number of occluded volumes in the material. System 3 contains a broader distribution of the occluded phase but a smaller total number. System 4 contains an even smaller number of occuded phases in the sample; system 5 has smaller occlusions and a larger number, but not quite as large as system 1. The improvement in the mechanical properties parallel these changes in morphology. System 2 with the smaller number of larger occlusions shows the least improvement in properties. Reducing the size of the occlusions, and increasing the number, leads to improvement in properties with systems 3 and 4 but do not match the behavior in system 1. These changes in behavior with composition reflect similar observations reported in a number of studies.[28–30] Studies on the physical properties of similar resin systems have been reported[29] and it has been observed that the fracture toughness increases with increase in molecular weight of the polystyrene in the system. Analysis of their data also indicates that the morphology is sensitive to the nature of the end groups and is optimum with amine termination. The chemical resistance of the matrix will be lost once a phase inverted structure is formed and the optimum properties are achieved in the cocontinuous region. These observations are consistent with those reported above for these systems and emphasize the importance of being able to monitor the nature of the phase structure during the curing process as indicated by the dielectric measurements.

The authors would like to thank the SERC and ICI plc for financial support (A.J.M.) and ICI plc for the provision of equipment, materials, test facilities, and overall support.

REFERENCES

1. C. B. Bucknall and I. K. Partridge, *Polym. Eng. Sci.*, **26**, 54 (1986).

2. C. B. Bucknall and I. K. Partridge, *Polymer,* **24,** 639 (1983).
3. C. B. Bucknall and A. H. Gilbert, *Polymer,* **30,** 213 (1989).
4. J. A. Cecere, J. S. Senger, and J. M. McGrath, 32nd Int. SAMPE Symp., 1987, p. 1276.
5. M. S. Sefton, P. T. McGrail, J. A. Peacock, S. P. Wilkinson, R. A. Crick, M. Davies, and G. Almen, 19th Int. SAMPE Tech. Conf., 1987, p. 700.
6. D. A. Shimp, F. A. Hudock, and W. S. Bobo, 18th Int. SAMPE Tech. Conf., 1986, p. 851.
7. H. D. Stenzenberger, W. Romer, M. Herzag, and P. Konig, 33rd Int. SAMPE Symp., 1988, p. 1546.
8. M. S. Sefton, P. T. McGrail, P. Eustace, M. Chisholm, J. T. Carter, G. Almen, P. D. MacKenzie, and M. Choate, 3rd Int. Conf. on Crosslinked Polymers, 1989.
9. K. Yamanaka and T. Inoue, *Polymer,* **30,** 662 (1989).
10. T. Ohnaga, J. Maruta, and T. Inoue, *Polymer,* **30,** 1845 (1989).
11. S. D. Senturia and N. F. Sheppard, *Adv. Polym. Sci.,* **80,** 1 (1986).
12. W. W. Bidstrup, N. F. Sheppard, and S. D. Senturia, *Polym. Sci. Eng.,* **26,** 358 (1986).
13. M. L. Bromberg, D. R. Day, and K. R. Snable, *Electr. Insul.,* **2,** 18 (1986).
14. Z. N. Sanjana, *Polym. Sci. Eng.,* **26,** 358 (1986).
15. W. X. Zukas, N. S. Schneider, and W. J. MacKnight, *Am. Chem. Soc. Div. Polym. Chem. Polym. Prepr.,* **25,** 205 (1984).
16. Z. N. Sanjana and R. L. Selby, Proc. 29th SAMPE Symp., 1984, p. 1233.
17. W. W. Bidstrup and S. D. Senturia, *Polym. Eng. Sci.,* **29,** 290 (1989).
18. A. J. MacKinnon, S. D. Jenkins, P. T. McGrail, and R. A. Pethrick, *Macromolecules,* **25,** 3492 (1992).
19. A. J. MacKinnon, S. D. Jenkins, P. T. McGrail, and R. A. Pethrick, *Polymer,* **34,** 3253 (1993).
20. A. J. MacKinnon, S. D. Jenkins, P. T. McGrail, and R. A. Pethrick, *Polymer,* to appear.
21. L. K. H. Van Beek, *Prog. Dielectr.,* **7,** 69 (1967).
22. D. Hayward, E. Trottier, A. Collins, S. Affrossman, and R. A. Pethrick, *J. Oil Col. Chem. Assoc.,* **11,** 452 (1989).
23. A. J. Barlow, A. Erginsav, and J. Lamb, *Proc. R. Soc. A,* **A309,** 473 (1969).
24. J. Cochrane and G. Harrison, *J. Phys. E,* **5,** 47 (1972).
25. M. Davies and D. R. Moore, *Comp. Sci. Technol.,* **40,** 131 (1991).
26. J. H. Daly, R. A. Pethrick, P. Fuller, and A. V. Cunliffe, *Polymer,* **22,** 33 (1981).
27. A. J. Kinloch, S. J. Shaw, D. A. Tod, D. L. Hunston, *Polymer,* **24,** 1341 (1983).
28. J. L. Hedrick, I. Yilgor, M. Yurek, J. C. Hedrick, G. L. Wilkes, and J. E. McGrath, *Polymer,* **32,** 2020 (1991).
29. S. J. Pak, G. D. Lyle, R. Mercier, and J. E. McGrath, *Polymer,* **34,** 885 (1993).
30. G. W. Meyer, Y. J. Lee, S. J. Pak, and J. E. McGrath, *ACS Polym. Prepr.,* **207,** (1994).

Received January 31, 1995
Accepted March 7, 1995